Supporting Information

Ultrasensitive airflow sensor prepared by electrostatic flocking for sound recognition and motion monitoring

Jin Luo,[a] Nan Ji,[a] Weiwei Zhang,[a] Pei Ge,[a] Yixuan Liu,[a] Jun Sun,[a] Jianjun Wang,[a] Qiqi Zhuo,[*b] Chuanxiang Qin[*a] and Lixing Dai[*a]

[a]College of Chemistry, Chemical Engineering and Materials Science, Soochow University, Suzhou 215123, P. R. China.
[b]College of Material Science & Engineering, Jiangsu University of Science and Technology, Zhenjiang, 212003, P. R. China.
[*]Corresponding author E-mail: dailixing@suda.edu.cn; qinchuanxiang@suda.edu.cn; zqq88263268@just.edu.cn

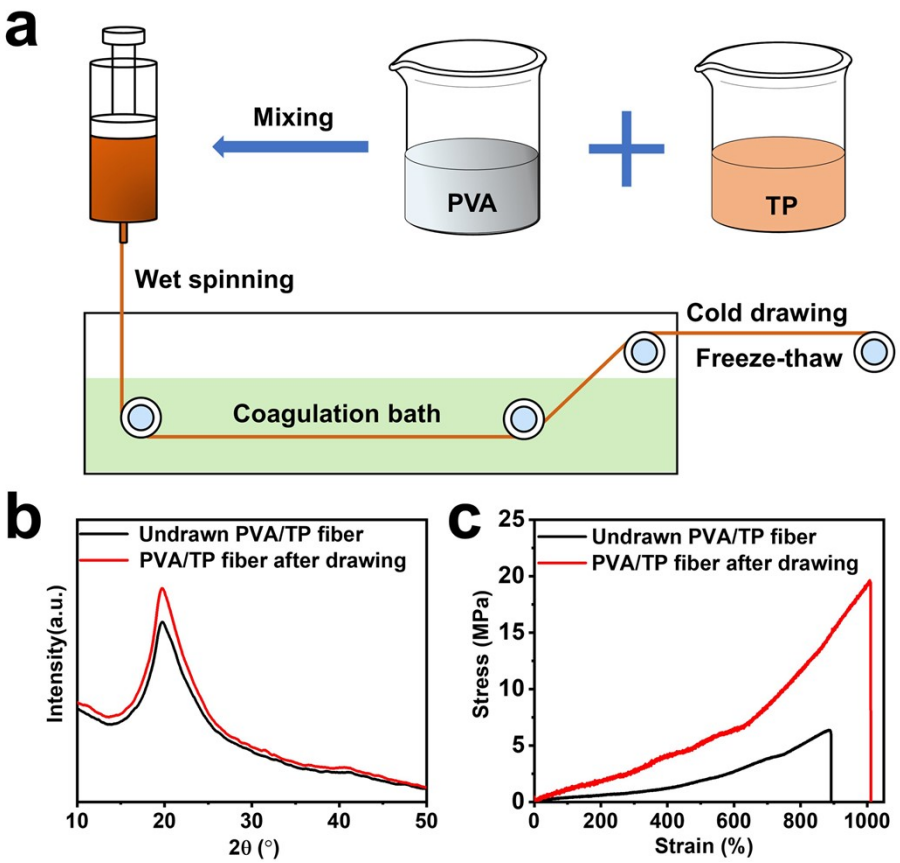

Figure S1. (a) Schematic illustration of the preparation process of PVA/TP hydrogel fiber. (b) XRD patterns and (c) tensile stress-strain curves of the undrawn and drawn PVA/TP hydrogel fibers.

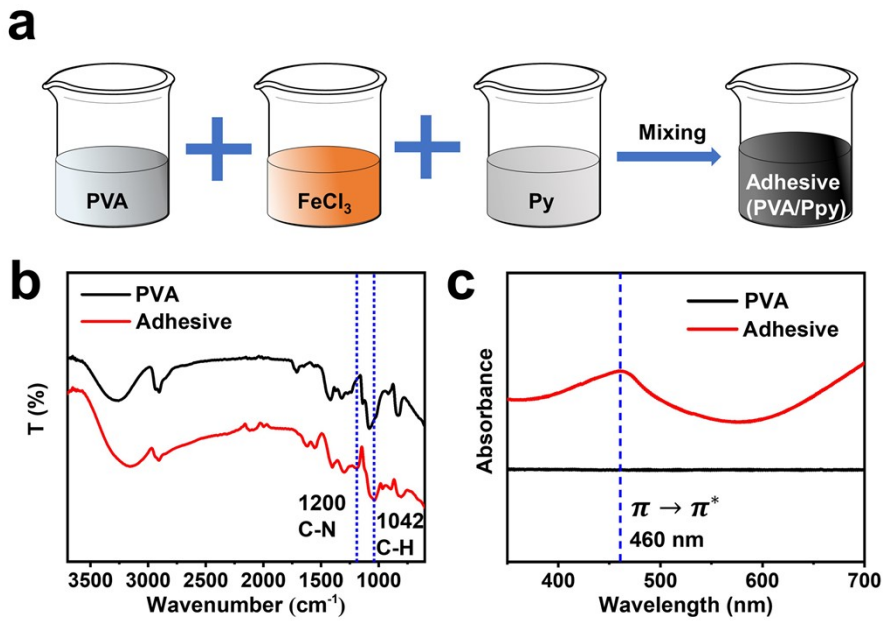

Figure S2. (a) Schematic illustration of the preparation process of adhesive (PVA/Ppy). (b) FT-IR spectra and (c) UV-vis spectra of pure PVA and adhesive.

Figure S2a illustration of the preparation process of adhesive. Figure S2b displays the ATR-FTIR spectra of pure PVA and the adhesive, compared with pure PVA, there are new peaks at 1200 cm^{-1} and 1040 cm^{-1} for the adhesive, which are suggested to be caused by the C-N stretching and C-H deformation vibration of Ppy.[1,2] Figure S2c shows the UV-vis spectra of PVA and the adhesive. The broad peaks over the range of 400–500 nm reveal the polymerization has happened, while peak summit present at 460

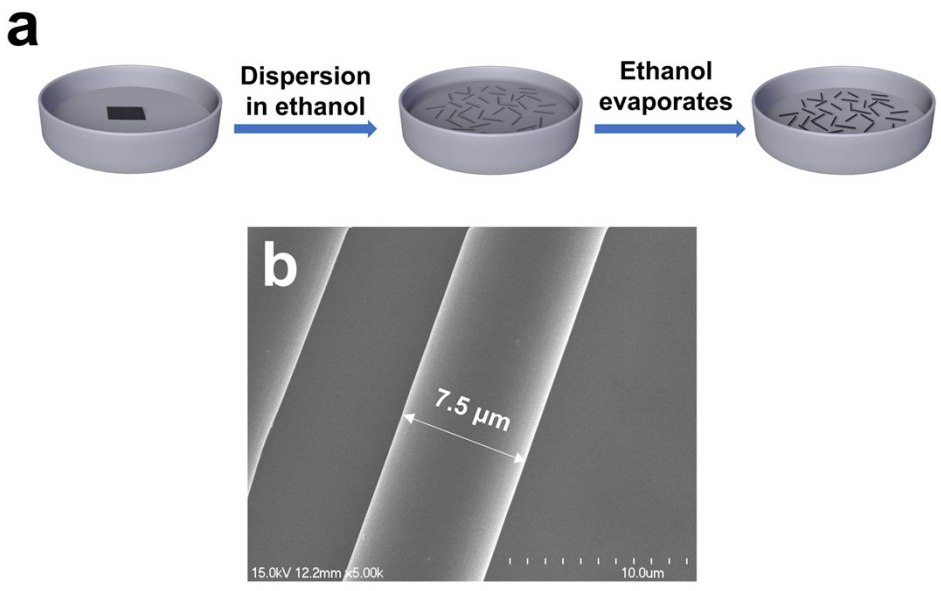

nm indicates completion of the polymerization of Ppy in the adhesive.[3,4]

Figure S3. (a) Treatment of CFs. (b) SEM of CFs.

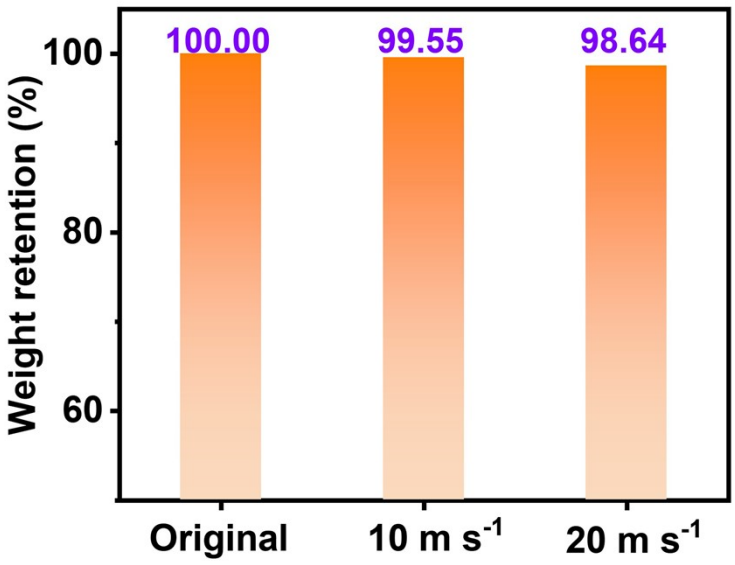

Figure S4. The weight retention of the sensor (1.57 mg cm^{-2}, 3 mm) after being blown with high velocities (10, 20 m s^{-1}) for 10 s.

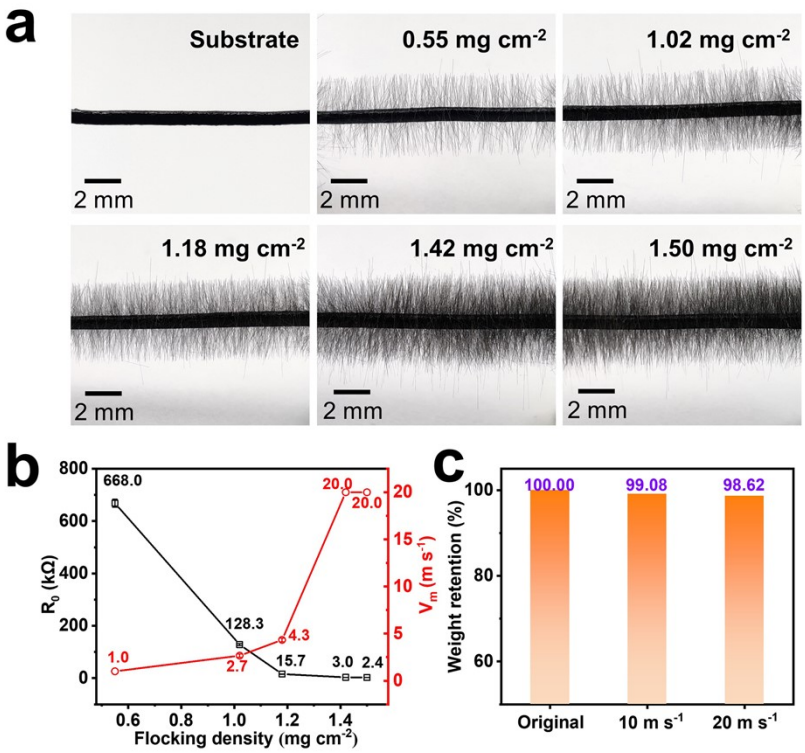

Figure S5. (a) Photographs of sensors at different flocking densities. (b) The resistance and the maximum allowable airflow velocity (V_m) of the sensors at different flocking densities. (c) The weight retention of the sensor (1.42 mg cm^{-2}) after being blown with high velocities (10, 20 m s^{-1}) for 10 s. The length of CFs of the sensors is 2 mm.

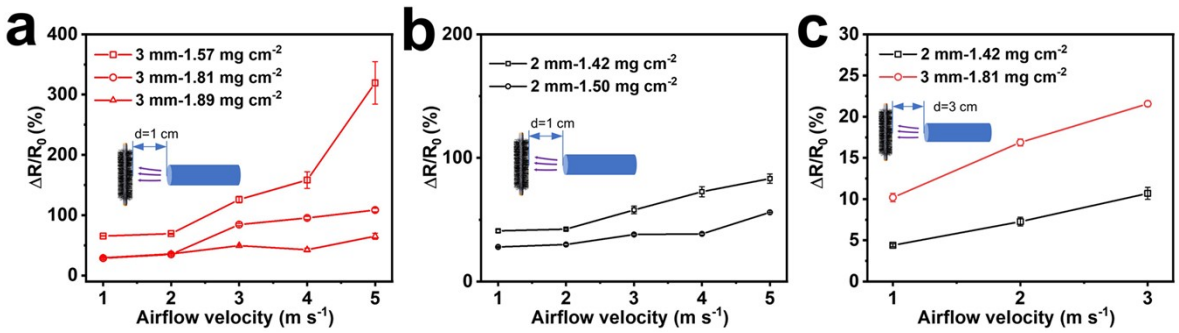

Figure S6. $\Delta R/R_0$ against airflow velocity of the sensors with the length of CFs (a) 3 mm, (b) 2 mm under different flocking densities when d is 1 cm. (c) $\Delta R/R_0$ against airflow velocity of two different sensors (2 mm-1.42 mg cm^{-2} and 3 mm-1.81 cm^{-2}) when d is 3 cm. d is the distance between the airflow pipeline and sensor.

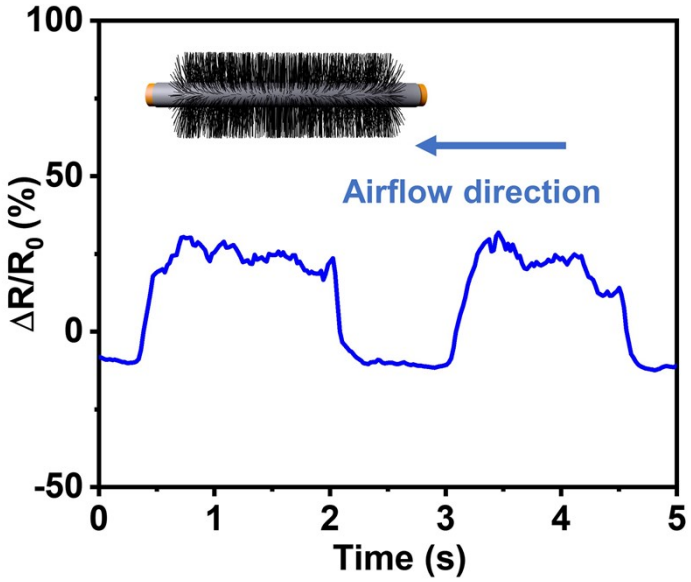

Figure S7. Two cyclic sensing curves of the sensor at airflow velocity of 1 m s^{-1} with parallel airflow directions.

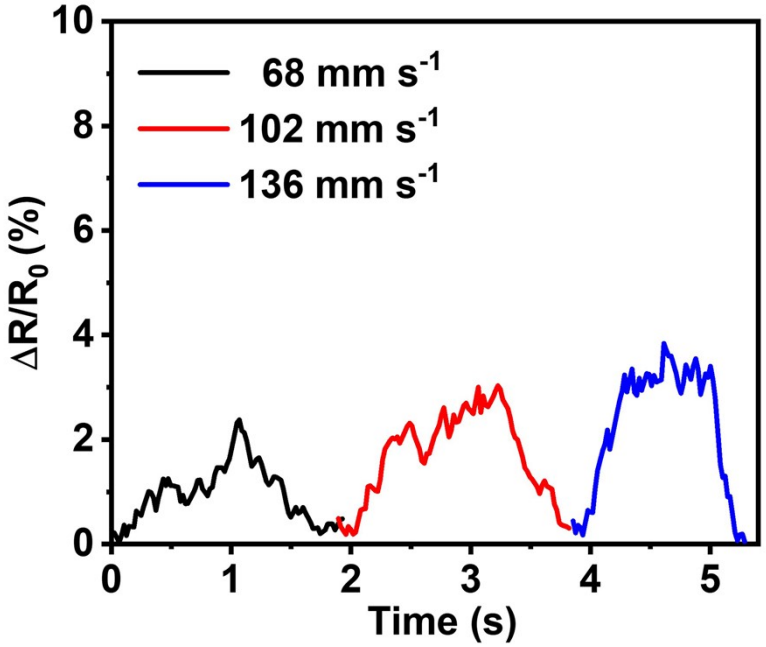

Figure S8. The responses curves of the sensor to ultralow airflow velocity.

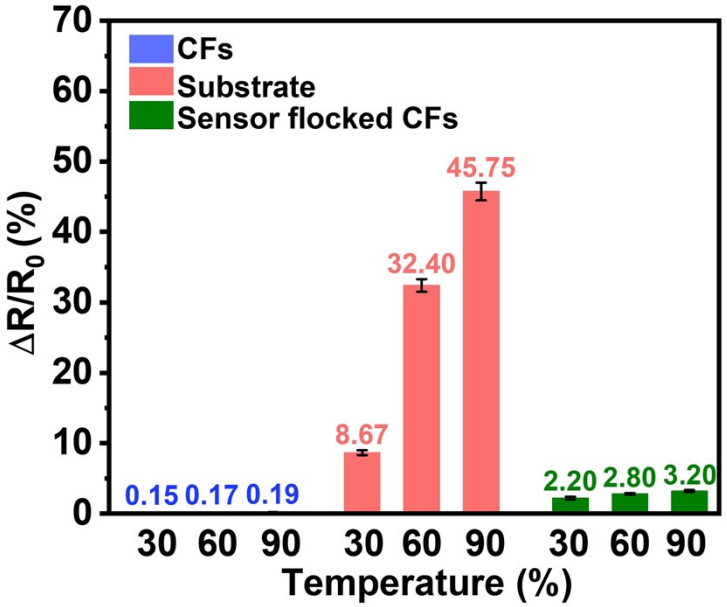

Figure S9. $\Delta R/R_0$ of CFs, substrate, and the sensor flocked CFs (1.81 mg cm^{-2}, 3 mm) placed under different temperature (30, 60, and 90 °C) for 20 s.

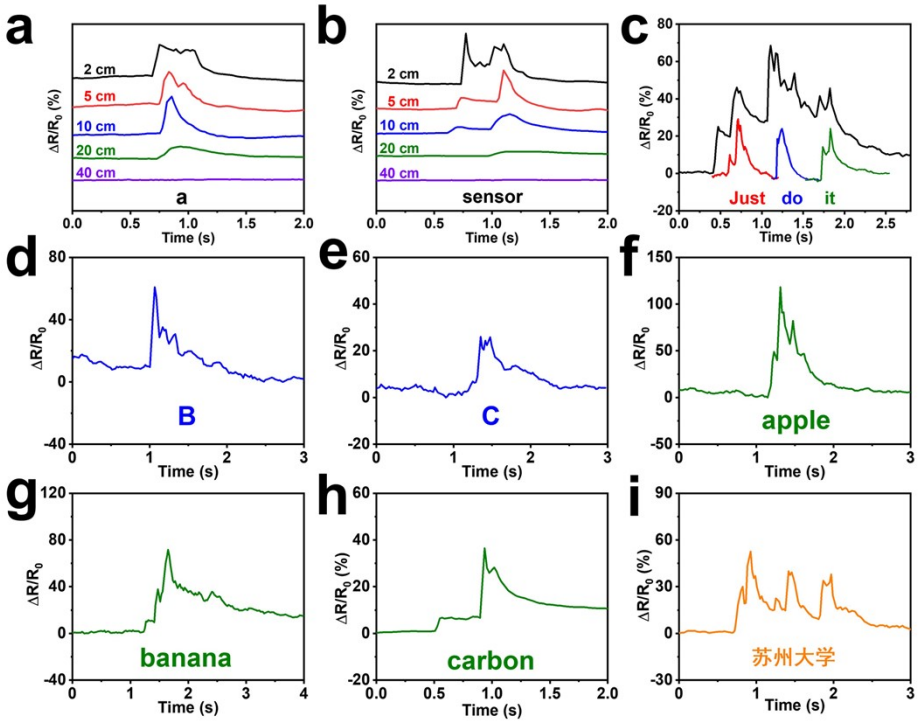

Figure S10. Response curves of the sensor when people speaking (a) 'a' and (b) 'sensor' in front of the sensor at different distances, (c) 'Just do it' continuously and separately, (d) 'B', (e) 'C', (f) 'apple', (g) 'banana', (h) 'carbon', and (i) '苏州大学' in front of the sensor.

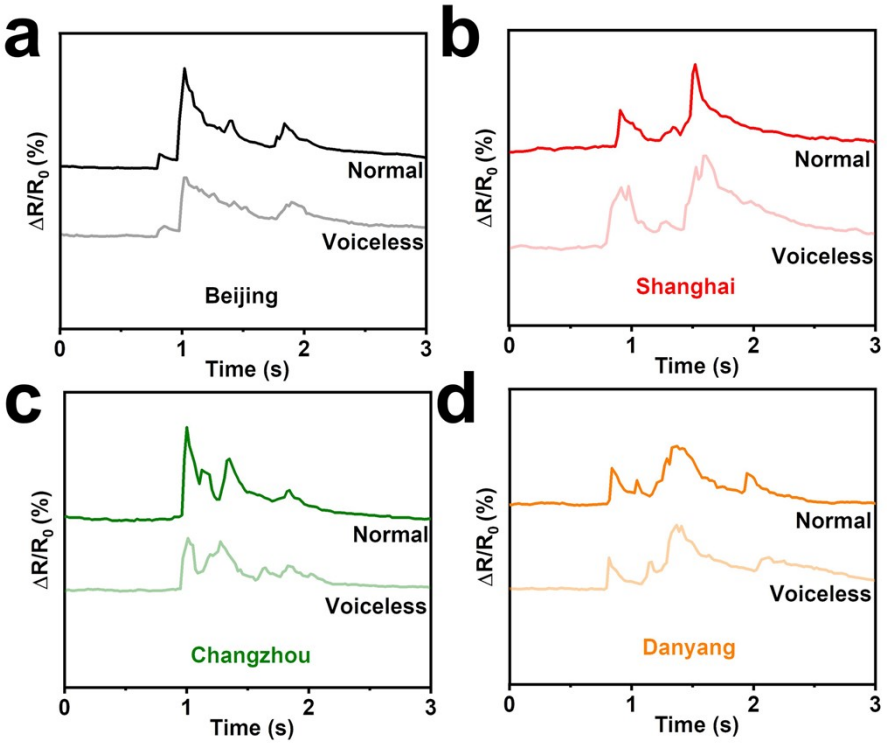

Figure S11. Recognition curves of the sensor to (a) 'Beijing', (b) 'Shanghai', (c) 'Changzhou', and (d) 'Danyang' in both cases of normal and voiceless speaking.

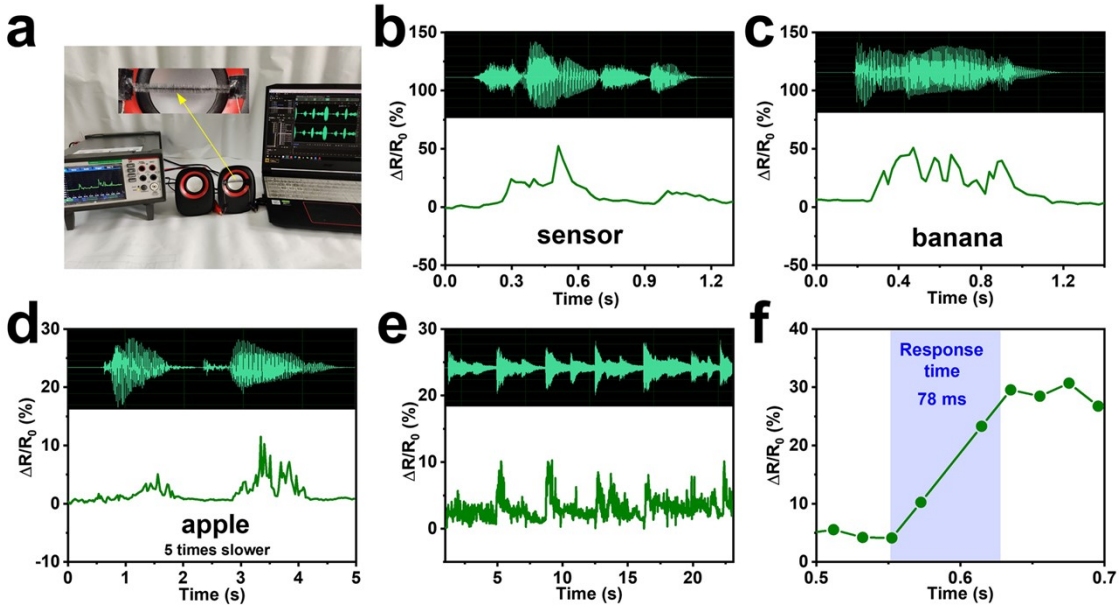

Figure S12. (a) Photograph of the sensor attached to the loudspeaker. The enlarged view of the sensor (arrow). $\Delta R/R_0$ curve (lower) and the corresponding sound wave diagram (upper) of the sensor when the loudspeaker playing (b) 'sensor', (c) 'banana', (d) 'apple' (5 times slower), and (e) part of the piano song 'Canon'. (f) Response time of the sensor to the sound.

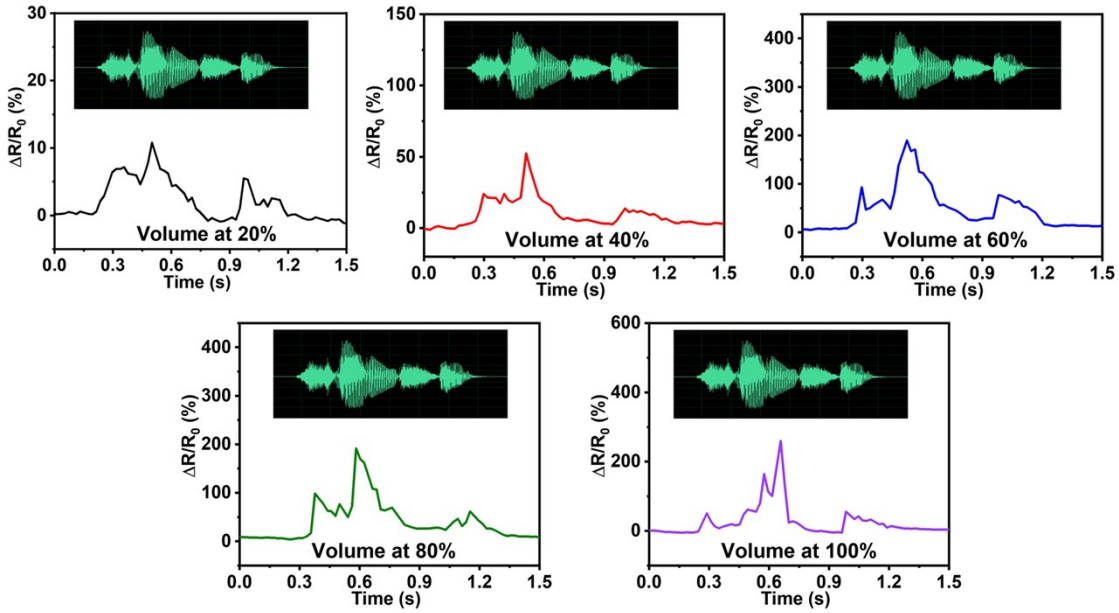

Figure S13. $\Delta R/R_0$ curve (lower) and the corresponding sound wave diagram (upper) of the sensor when the loudspeaker playing 'sensor' at different volume levels.

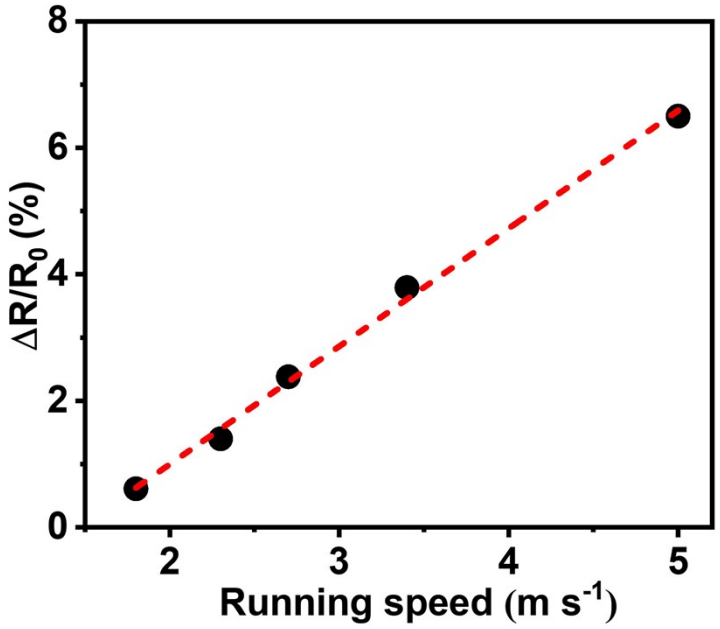

FigureS14. $\Delta R/R_0$ of the sensor to running at different speeds.

Table S1. Key parameters of the reported airflow sensors

Record	Materials	Principle	Sensitivity	Detection range	Response time	Ref.
1	CNTs/CSF	Piezoresistive	0.41 % s m^{-1} (1–3 m s^{-1})	0.05–7 m s^{-1}	1.3 s	5
2	CNTs/RGO film	Piezoresistive	0.2 % s m^{-1} (0.1–3.5 m s^{-1})	0.0176–3 m s^{-1}	1.04 s	6
3	PEDOT: PSS fibers	Piezoresistive	0.12 % s m^{-1}	0.5–3.5 m s^{-1}	0.27 s	7
4	RGO film	Piezoresistive	2.08 % s m^{-1} (0.026–8 m s^{-1})	0.026–7.2 m s^{-1}	26 s	8
5	Single Silicon Nanowires	Piezoresistive	0.131 % s m^{-1} (0.15–15.3 m s^{-1})	0.04–15.3 m s^{-1}	0.04 s	9
6	Bioinspired Carbon Nanotube	Piezoresistive	1.3–1.8% s m^{-1}	1–10 m s^{-1}	0.4 s	10
7	Vertical carbon fibers	Piezoresistive	24.7 % s m^{-1} (1–8 m s^{-1}) 90.4 % s m^{-1} (8–16 m s^{-1})	0.068–16 m s^{-1}	0.103 s	This work

Notes and references

1 W.-D. Lin, H.-M. Chang and R.-J. Wu, *Sens. Actuators, B*, 2013, **181**, 326-331.
2 N. Van Hieu, N. Q. Dung, P. D. Tam, T. Trung and N. D. Chien, *Sens. Actuators, B*, 2009, **140**, 500-507.
3 R.-J. Wu, Y.-C. Huang, M. Chavali, T. H. Lin, S.-L. Hung and H.-N. Luk, *Sens. Actuators, B*, 2007, **126**, 387-393.
4 P. Rapta, R. Faber, L. Dunsch, A. Neudeck and O. Nuyken, *Spectrochimica Acta Part a-Molecular and Biomolecular Spectroscopy*, 2000, **56**, 357-362.
5 H. Wang, S. Li, Y. Wang, H. Wang, X. Shen, M. Zhang, H. Lu, M. He and Y. Zhang, *Adv Mater*, 2020, **32**, 1908214.
6 W. Zhou, P. Xiao, Y. Liang, Q. Wang, D. Liu, Q. Yang, J. Chen, Y. Nie, S. W. Kuo and T. Chen, *Adv. Funct. Mater.*, 2021, **31**, 131551.
7 P. Wang, M. X. Wang, J. D. Zhu, Y. H. Wang, J. F. Gao, C. X. Gao and Q. Gao, *Chem. Eng. J.*, 2021, **425**, 131551.
8 Z. Y. Xu, K. J. Wu, S. N. Zhang, Y. C. Meng, H. W. Li and L. Q. Li, *Mater. Horiz.*, 2017, **4**, 383-388.
9 S. Huang, B. Zhang, Y. Lin, C. S. Lee and X. Zhang, *Nano Lett*, 2021, **21**, 4684-4691.
10 M. R. Maschmann, G. J. Ehlert, B. T. Dickinson, D. M. Phillips, C. W. Ray, G. W. Reich and J. W. Baur, *Adv Mater*, 2014, **26**, 3230-3234.